

# HYBRID MESON PRODUCTION VIA PION SCATTERING FROM THE NUCLEAR COULOMB FIELD

*Murray Moinester*

R. and B. Sackler Faculty of Exact Sciences, School of Physics and Astronomy, Tel Aviv University, 69978 Tel Aviv, Israel; e-mail: murraym@tauphy.tau.ac.il

## **Abstract**

The CERN COMPASS experiment can use 100–280 GeV pion and kaon beams and magnetic spectrometers and calorimeters to measure Hybrid (mixed quark–gluon) meson production cross sections in the Primakoff scattering of high-energy pions and kaons from virtual photons in the Coulomb field of high- $Z$  targets. There are many advantages to studying such processes via the Primakoff reactions  $\pi^- \gamma \rightarrow Hybrid \rightarrow \rho\pi, \eta\pi, \eta'\pi, \pi b_1, \pi f_1$ , and similar reactions with a  $K^-$  beam. Such data should provide significant input for gaining a better understanding of non-perturbative QCD. A brief description and update of this programme is presented.

## **1. PIONIC HYBRID MESONS**

The CERN COMPASS experiment focuses on issues in the physics of strong interactions pertaining to the structure of hadrons in terms of valence quarks and gluons. This report deals with the COMPASS Hybrid meson programme. The Hybrid (quark–antiquark–gluon,  $q\bar{q}g$ ) mixed quark–gluon mesons are particles predicted by QCD [1–4]. The unambiguous discoveries of these meson states will provide a major landmark in hadron spectroscopy. Of course, the Fock state of a meson is represented as an infinite expansion of different quark and gluon configurations, but in a Hybrid meson, the  $q\bar{q}g$  component dominates. The force between quarks in QCD is mediated by the exchange of coloured gluons. In ordinary quark–antiquark mesons, the exchanged gluons localize within a narrow string-like tube connecting the quarks: a non-vibrating flux-tube of coloured flux lines. In the flux-tube description of a Hybrid meson, a quark–antiquark pair couples directly to the vibrational degrees of freedom of the gluonic flux-tube. Hybrid mesons therefore contain explicit valence gluons, as opposed to the hidden gluons in ordinary mesons [3]. Understanding such valence gluons is critical to understanding the origin of hadron mass. Establishing the existence of Hybrid mesons and studying their properties can provide insight into colour confinement.

Input from experiments is needed to provide better understanding of the current situation, especially to show that the present evidence [5] is not just the result of some artifice. GSI Darmstadt [6] proposes an exotic meson programme via a new facility for  $p\bar{p}$  reactions. The planned \$150M 12 GeV JLab upgrade focuses on Hybrid meson studies at JLab Hall D [7]. Future experiments at Fermilab CDF and D0 may measure double-Pomeron production of exotic mesons [8]. More results from BNL, VES, Crystal Barrel [9–11] (from analysis of completed experiments), and further theoretical calculations, are becoming available. COMPASS has a multi-faceted Hybrid meson research programme [12, 13], which includes this proposal for Primakoff production of Hybrids. COMPASS [14] is well positioned to collect significantly cleaner data, and at lower cost, and using complementary methods, compared to the other planned efforts. The Primakoff production of Hybrids in COMPASS is part of a more global Primakoff physics programme, involving studies of pion and kaon polarizabilities, and studies of the chiral anomaly [14, 15].

The COMPASS Hybrid meson searches [15–17] will focus on ‘oddballs’—mesons with quantum numbers not allowed for ordinary  $q\bar{q}$  states, such as  $I^G J^{PC} = 1^- 1^{-+}$  Hybrids. Unlike Glueballs, these cannot mix with normal  $q\bar{q}$  mesons. However, since such oddballs could also be four-quark states, the

spin assignment is not sufficient to make the Hybrid identification [18]. In certain cases, there are other theoretical interpretations [19, 20] for such experimental signals. Previous experimental efforts have reported several  $1^{-+}$  resonant signals [9–11] at masses between 1.4 and 1.9 GeV, in a variety of decay channels, including the  $\rho\pi$  channel. The signature for such an exotic state is that a detailed partial-wave analysis (PWA) of a large data sample requires a set of quantum numbers inconsistent with a normal ( $q\bar{q}$ ) meson. To increase confidence in a Hybrid interpretation, complementary evidence is sorely needed. The path to understanding requires that different experiments, such as the important input from COMPASS Primakoff studies, provide a large database of candidate Hybrid states, and their properties.

Barnes and Isgur, using the flux-tube model [21, 22], calculated the mass of the lightest pionic hybrid with quantum numbers of  $J^{PC} = 1^{-+}$  to be around 1.9 GeV, higher than the experimental claims. Close and Page [23] predict that such a high-lying pionic hybrid should decay into the following channels:

$$\begin{array}{c|c|c|c|c} b_1\pi & f_1\pi & \rho\pi & \eta\pi & \eta'\pi \\ \hline 170 & 60 & 5 \rightarrow 20 & 0 \rightarrow 10 & 0 \rightarrow 10 \end{array}$$

where the numbers refer to the partial widths in MeV. They expect the total width to be larger than 235–270 MeV, since the  $s\bar{s}$  decay modes were not included. Recent updates on hybrid meson structure are given in Refs. [3, 24, 25]. The lower lying Hybrids of recent experiments have significantly different branching ratios. This may reflect that the structure of these experimental low-mass Hybrids is different than that of the theoretical high-mass Hybrids, and considering the high thresholds of the  $b_1\pi$  and  $f_1\pi$  decay channels for decay of a low-mass Hybrid.

From over a decade of experimental efforts at IHEP [26–28], CERN [9, 29], KEK [30], and BNL [10], several hybrid candidates have been identified. BNL E852 [10] reported two  $J^{PC} = 1^{-+}$  resonant signals at masses of 1.4 and 1.6 GeV in  $\eta\pi^-$  and  $\eta\pi^0$  systems, as well as in  $\pi^+\pi^-\pi^-$ ,  $\pi^-\pi^0\pi^0$ ,  $\eta'\pi^-$  and  $f_1(1285)\pi^-$ . The VES Collaboration presented [11] the results of a coupled-channel analysis of the  $\pi 1(1600)$  meson in the channels  $b_1(1235)\pi$ ,  $\eta'\pi$ , and  $\rho\pi$ , with a total width of 290 MeV, and relative branching ratios:  $1 : 1 \pm 0.3 : 1.6 \pm 0.4$ . They did not include the  $f_1\pi$  channel in this analysis. The resonant nature of the 1.6 GeV state was observed in the  $b_1\pi$  mode, by a combined fit of the  $2^{++}$  and  $1^{-+}$  waves. Then an assumption was made that in the  $\eta'\pi$  and  $\rho\pi$  channels, they observed the same state, considering the similar shapes. Therefore, their coupled-channel analysis result of a  $\rho\pi$  partial width of 130 MeV, and a total width of 290 MeV, should be taken with some caution, considering also that the  $f_1\pi$  channel is not included. Still, for the 1.6 GeV region, the VES  $\rho\pi$  partial width is consistent with the BNL  $\rho\pi$  width of 168 MeV. For count rate estimates below, we will use an average value of 150 MeV for the  $\rho\pi$  width at 1.6 GeV.

The kinematic variables for the  $\pi\gamma \rightarrow \text{Hybrid} \rightarrow \pi^-\eta$  Primakoff process in COMPASS are shown in Fig. 1. A virtual photon from the Coulomb field of the target nucleus interacts with the pion beam. At 200 GeV  $\pi$  beam energy, nuclear (meson-exchange) amplitudes in the Primakoff production of the  $\rho$  meson were shown to be very small [31] in the kinematic region of Primakoff production. This is very encouraging for the COMPASS studies. Still, COMPASS can carry out data analysis of Hybrid data with and without meson-exchange amplitudes, to test to what extent their presence affects the extraction of the Primakoff cross section. For a given Hybrid ( $\pi 1$ ) partial decay width  $\Gamma(\pi 1 \rightarrow \pi\rho)$ , the Vector Dominance Model (VDM) gives an associated radiative width  $\Gamma(\pi 1 \rightarrow \pi\gamma)$  [32, 33]. As the Primakoff cross section is proportional to  $\Gamma(\pi 1 \rightarrow \pi\gamma)$  [32–34], all Hybrids that decay to the  $\pi\rho$  channel should also be produced in the Primakoff reaction. In contrast to the  $\pi 1(1600)$ , the  $\pi 1(1400)$   $1^{-+}$  state should be only weakly populated in the Primakoff reaction, as it has a very small  $\pi\rho$  partial decay width. For the  $\pi 1(1600)$  radiative width, we use the standard VDM expression [31–33] with a  $\rho\gamma$  coupling  $g_{\rho\gamma}^2/\pi = 2.5$ , which correctly relates the corresponding widths for the  $\rho$  meson decay. We obtain  $\Gamma(\pi 1 \rightarrow \pi\gamma) = 6.6 \times 10^{-3}\Gamma(\pi 1 \rightarrow \pi\rho)$ , which gives the VDM estimate  $\Gamma(\pi 1 \rightarrow \pi\gamma) \approx 1000$  keV.

In Fig. 1, a Hybrid meson (other than  $\pi 1(1400)$ ) is produced and decays to  $\pi^-\eta$  at small forward

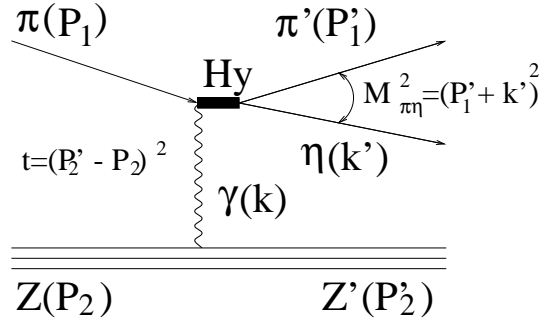


Fig. 1: Primakoff Hybrid-meson production process and kinematic variables (4-momenta):  $P_1, P_1'$  = for initial/final pion,  $P_2, P_2'$  = for initial/final target,  $k$  = for initial  $\gamma$ ,  $k'$  = for final  $\eta$ .

angles in the laboratory frame, while the target nucleus (in the ground state) recoils coherently with a small transverse  $p_T$ . The corresponding small  $p_T$  of the exchanged photon means that it is essentially real and transverse. Consequently, the helicities of incident and Primakoff produced mesons differ by unity. The peak at small target  $p_T$  used to identify [32, 33] the Primakoff process is observed by using the beam and vertex and other COMPASS detectors to measure the beam-pion and final-state Hybrid momenta. Primakoff scattering is a large impact-parameter, ultra-peripheral reaction on a virtual photon target. The initial-state pion and final-state Hybrid interact at very small  $t$ -value (four-momentum transfer to the target nucleus), where the nuclear form factor is essentially unity, and there are no final-state interactions [35].

It is important to note that in addition to Primakoff production of excited meson states, one also expects diffractive production. It is necessary to separate the Primakoff forward peak from these underlying sometimes large diffractive yields [32, 34]. The strength of the diffractive cross section depends on angular momentum conservation at zero degrees; and therefore on which decay mode is studied:  $b_1\pi$ ,  $f_1\pi$ ,  $\rho\pi$ ,  $\eta\pi$ ,  $\eta'\pi$ . The potentially large diffractively produced waves with spin projection  $M = 0$  and  $J^P = 1^+$  can complicate the PWA of  $\rho\pi$ , but not  $\pi\eta$ . Of course, although the  $\pi\eta$  channel may be cleaner, it may not necessarily have a large  $1^-$  Hybrid contribution.

The  $t$ -distribution of the diffractive yield depends on whether there is helicity flip at zero degrees. The  $t$ -dependence of these dominant (no helicity-flip) diffractive waves is  $\exp(-bt)$ . The accuracy with which one can subtract this background depends on the fraction of the projective helicity-flip ( $M = \pm 1$ ) diffractive waves associated with  $2^+$  states, which have a  $t$ -dependence  $t \times \exp(-bt)$ . All the waves have phases and can interfere, so that subtracting only an exponential would ignore these effects. However, as the Coulomb waves have Gottfried–Jackson helicity  $M = \pm 1$ , while strong production occurs dominantly with  $M = 0$ , the interference should be zero to lowest order [36].

Such subtraction was done, even for a large diffractive cross section [36], as in the recent measurement of the radiative decay width of the  $a_2(1320)$  meson [34] via its decay to the  $\pi\rho$  channel. The subtraction was done by extrapolation of the data away from the forward Primakoff peak, assuming an  $\exp(-bt)$  dependence of the diffractive yields. Such theoretical assumptions on the  $t$ -dependence of the background should have a small effect on narrow resonances (104 MeV width) such as the  $a_2$ . This appears to be the case, considering the consistency of the  $a_2$  radiative widths determined via Primakoff production and their decay via the  $\pi\rho$  and  $\pi\eta$  channels [34]. But an exponential subtraction may cause larger uncertainties for Hybrids with large (300–500 MeV) widths. The Hybrid data analysis therefore should test the sensitivity of the results to such exponential background assumptions.

In the recent Primakoff study of the  $a_2$  radiative width by decay to  $\pi\rho$ , following subtraction of the diffractive yield, due in part to poor statistics, the resulting Primakoff mass spectrum does not show significant structure above the clearly observed  $a_2(1320)$ . Also, for this high mass region, a PWA is not

available. Considering the subtraction and statistical uncertainties discussed above, this does not rule out the possibility that the  $\pi\rho$  width is nonetheless large in the region of the expected 1.6 GeV Hybrid. And with improved statistics and resolution and acceptance, and by studying all decay modes in the same experiment, COMPASS can potentially do a significantly better Hybrid analysis. High-lying excited meson states certainly couple to the  $\pi\rho$  channel, as shown clearly in the work of photoproduction of excited mesons, observed by their  $\pi\rho$  decay mode [37].

Consider some typical angular distributions from Primakoff scattering, such as those for the  $\pi^-\gamma \rightarrow \eta\pi$  scattering, for different values of  $\eta\pi$  invariant mass. If these are associated with the production and decay of a  $J^{PC} = 1^{-+}$  ( $d\bar{u}g$ ) Hybrid state, with quantum numbers not available to  $q\bar{q}$  mesons, then a detailed partial-wave analysis (PWA) of a large data sample would indicate the need for these quantum numbers. The partial-wave analysis (PWA) of systems such as  $\eta\pi$  or  $\eta'\pi$  in the mass region below 2 GeV requires high statistics and minimum background. This region is dominated by strong resonances (e.g.,  $a_2(1320)$  near the 1.4 GeV Hybrid candidate and  $\pi_2(1670)$  near the 1.6 GeV Hybrid candidate), and the PWA can yield ambiguous results [27] for the weaker  $1^{-+}$  wave. For the Primakoff yield, following subtraction of the diffractive yield, the cross section for 1.6 GeV hybrid production ( $\pi 1$ ), in all decay channels, should be larger than the background. This is so because  $\Gamma(\pi_2 \rightarrow \pi\gamma) \approx 300$  keV, smaller than the expected  $\Gamma(\pi 1 \rightarrow \pi\gamma) \approx 1000$  keV. In contrast, the BNL experiment [10] for this decay channel has a background from  $\pi_2(1670)$  some 10 times stronger than the Hybrid signal. Primakoff data with reduced backgrounds should significantly diminish uncertainties in the partial wave analysis compared to the non-Primakoff production experiments. It might allow the Hybrid to be observed in the mass spectrum in some of the decay modes, not only via PWA. Furthermore, in Primakoff (photon-exchange) production experiments, besides the absence of final-state interactions, meson-exchange and diffractive backgrounds can be largely eliminated. Most of these backgrounds occur at larger values of the four-momentum transfer  $t$ , and are easily removed by an analysis cut on the  $t$ -value. The part of these backgrounds that extends to small- $t$  can be largely removed by extrapolation to small- $t$  of the large- $t$  data. These are important advantages compared to previous  $\pi^-p \rightarrow \text{Hybrid}$  production experiments [16, 17].

Preliminary low-statistics Hybrid production data [32, 33] at Fermilab E272 via Primakoff scattering provide encouraging initial results for production of a 1.6 GeV  $1^{-+}$  Hybrid. The data for decay to the  $\pi f_1$  channel shows signs of Primakoff enhancement (excess of 25 events) at small- $t$ . This gives  $\Gamma(\pi 1 \rightarrow \pi\gamma) \times B(\pi 1 \rightarrow \pi f_1) \approx 250$  keV. If  $B(\pi 1 \rightarrow \pi f_1) \approx 0.25$ , that corresponds to  $\Gamma(\pi 1 \rightarrow \pi\gamma) \approx 1000$  keV, close to the value deduced using VDM with a 150 MeV partial width in the  $\pi\rho$  channel. For  $\pi\rho$  decay of a 1.6 GeV state, FNAL E272 had insufficient statistics to separate a Coulomb enhancement from the diffractive background. As their data was for the combined spectra, their estimate of the upper limit to the Primakoff Hybrid yield has large uncertainties. FNAL SELEX measured the  $a_2$  radiative decay via the  $\pi\rho$  mode. The SELEX Primakoff spectrum, after subtraction of diffractive background, shows the  $a_2$  peak clearly. The E272  $\pi\rho$  data for diffractive plus Primakoff production does not even show the  $a_2$  peak. It is difficult to use E272 data to get Primakoff limits in the  $\pi\rho$  channel near 1.6 GeV. For a 150 MeV  $\pi\rho$  partial width of a 1.6 GeV Hybrid, the E272 data gives an upper limit for  $\Gamma(\pi 1 \rightarrow \pi\gamma)$  close to 100 keV. Since this limit value has a huge error bar, the E272 estimate using the cleaner  $\pi f_1$  data is certainly more reliable. E272 also shows via the  $\eta\pi$  decay mode, that  $\Gamma(\pi 1 \rightarrow \pi\gamma) \times B(\pi 1 \rightarrow \pi\eta)$  is at most 100 keV for a  $\pi 1$  near 1.6 GeV, for a  $\pi 1$  with a total width of 400 MeV. But the  $\pi 1$  branching  $B(\pi 1 \rightarrow \pi\eta)$  from VES and BNL is very small, so this is still consistent with  $\Gamma(\pi 1 \rightarrow \pi\gamma)$  near 1000 keV. Consequently, one may estimate from the E272  $\pi f_1$  data that  $\Gamma(\pi 1 \rightarrow \pi\gamma)$  is close to 1000 keV. This is consistent with  $\Gamma(\pi 1 \rightarrow \pi\gamma) \approx 1000$  keV, which we obtain by applying VDM to the experimental  $\Gamma(\pi 1 \rightarrow \pi\rho)$  width, as described above.

One can summarize the situation as follows. For Primakoff scattering, the Hybrid-meson production cross section depends on the strength of its  $\pi\rho$  coupling, and via vector dominance to its  $\pi\gamma$  coupling. Both BNL and VES claim this decay mode for the 1.6 GeV Hybrid candidate. A low-statistics  $\gamma p \rightarrow \text{Meson}$  photoproduction experiment [37] also observed resonances (including near 1.9 GeV) in the

$\pi\rho$  channel, suggesting possible Hybrid interpretations. Based on previous data from FNAL E272 and VES, we estimate  $\Gamma(\pi 1 \rightarrow \pi\gamma) \approx 1000$  keV for a 1.6 GeV Hybrid. The relevant Primakoff reactions  $\pi^- \gamma \rightarrow \text{Hybrid} \rightarrow \rho\pi, \eta\pi, \eta'\pi, b_1(1235)\pi, \pi f_1$ , etc., can therefore be studied in COMPASS potentially in the 1.4–3.0 GeV mass region, which includes all previous Hybrid candidates.

## 2. KAONIC HYBRID MESONS

The quark content of the hybrid meson ( $q\bar{q}g$ ) nonet should be identical to the quark content of the regular meson ( $q\bar{q}$ ) nonet, with identical SU(3) decomposition in the plane of isospin  $I_3$  and hypercharge  $Y$ , for the  $1^-$  and other spin-parity states. Thus, for every pionic ( $d\bar{u}g$ )  $1^{-+}$  Hybrid, there should be a flavour excited kaonic ( $s\bar{u}g$ )  $1^-$  Hybrid, at an excitation energy roughly 100–140 MeV higher than its pionic Hybrid cousin, possibly narrower because of phase space. COMPASS can observe the kaonic Hybrids via  $K^- Z \rightarrow \text{Hybrid} \rightarrow K^- \rho^0 Z$ , as well as other decay modes:  $b_1 K^-, f_1 K^-, \eta K^-, \eta' K^-$ . The backgrounds should be low from Primakoff excitation of normal kaonic excited mesons, as in the case of the pionic Hybrids; and also if the kaonic hybrids are narrower. The first ever measurement of the kaonic Hybrids via Primakoff scattering would be of inherent interest, but would also provide valuable support that the analogous pionic signals are properly identified as Hybrids. Searches for  $s\bar{s}g$  Hybrids via  $K^- p \rightarrow \text{Hybrid}$  have also been proposed recently [38].

## 3. MESON RADIATIVE TRANSITIONS

COMPASS will also study Primakoff radiative transitions leading from the pion to the  $\rho^-$ ,  $a_1(1260)$ , and  $a_2(1320)$ , and for the kaon to  $K^*$ . The data can be obtained with a particle-multiplicity trigger [17]. Theoretical predictions for radiative transition widths are available from vector dominance and quark models. Independent and higher precision data for these and higher resonances would provide a useful check of the COMPASS apparatus, and would allow a more meaningful comparison with theoretical predictions. For example, the  $\rho \rightarrow \pi\gamma$  width measurements [31, 39, 40] range from 60 to 81 keV; the  $a_1(1260) \rightarrow \pi\gamma$  width measurement [41] is  $0.64 \pm 0.25$  MeV; and the  $a_2(1320) \rightarrow \pi\gamma$  width is  $\Gamma = 295 \pm 60$  keV [42] and  $\Gamma = 284 \pm 25 \pm 25$  keV [34]. For  $K^* \rightarrow K\gamma$ , the widths obtained previously are  $48 \pm 11$  keV [43] and  $51 \pm 5$  keV [44]. The above references indicate that the formalism of Primakoff production provides an excellent description of excited mesons, the same formalism that we use to search for Primakoff production of Hybrids.

These as well as polarizability and chiral anomaly [14, 15] Primakoff measurements are important for a variety of reasons: (1) COMPASS can significantly improve their precision, (2) COMPASS can get data for other  $q\bar{q}$  meson excited states, (3) these measurements with sufficient statistics test our methodologies and help calibrate our apparatus for the Hybrid studies.

## 4. DETAILED DESCRIPTION OF APPARATUS

COMPASS is a fixed-target experiment that uses a 160 GeV polarized muon beam, and pion, kaon, and proton beams. In order to achieve good energy resolution within a wide energy range, COMPASS has a two-stage spectrometer with 1.0 Tm and 5.2 Tm conventional magnets. The tracking stations contain different detector types to cover a large area, and to achieve good spatial resolution in the vicinity of the beam. Most of the tracking detectors operate on the principle of gas amplification, while some are silicon strip detectors. At the end of each stage, an electromagnetic and a hadronic calorimeter detect energies of photons, electrons and hadrons. The calorimeters in the first stage and the EM calorimeter of the second stage have holes through which the beam passes.

In COMPASS, two beam Cherenkov detectors (CEDAR), far upstream of the target, provide  $\pi/K/p$  particle identification (PID). The incoming hadron momentum is measured in the beam spectrometer. Before and after the target, charged particles are tracked by high-resolution silicon tracking detectors. The measurement of both initial and final-state momenta provides constraints to identify the

reaction. The final-state meson momenta are measured downstream in the magnetic spectrometer and in the  $\gamma$  calorimeter. These provide a precise determination of the  $p_T$  transfer to the target nucleus, the main signature of the Primakoff process, and the means to separate Primakoff from meson-exchange scattering events.

We considered in detail previously the beam, target, detector, and trigger requirements for Hybrid studies [15, 17]. A brief description is given below of some important components of the apparatus for Primakoff studies. The September 2002 status of the full COMPASS apparatus is described in Ref. [35].

#### 4.1 Beam requirements

We can obtain good statistics for the pion study by using the high beam intensities of the CERN SPS. We can take data at different beam energies and use different targets, with both positive and negative beams, as part of efforts to control systematic uncertainties.

For the 120–300 GeV hadron beams, particle identification (PID) is needed to provide pion, kaon, and proton beam tagging for positive and negative beams. For the COMPASS beam, one expects [14] a beam intensity of 100 MHz, with beam composition [45] roughly: 120–300 GeV/ $c$ , negative, 87–98% pions, 7–1% kaons, 2–1% antiprotons; 120–300 GeV/ $c$ , positive, 43–2% pions, 7–1% kaons, 49–97% protons. PID is accomplished at CERN with the CEDAR detectors, a Cherenkov differential counter with achromatic ring focusing. There are two CEDAR detectors (in series) in the COMPASS beamline [46]. They each have eight large-area PMTs arranged in a circle, preceded by a single light diaphragm (LD) to finely fix a ring radius. A six-fold coincidence is required for the PID. The gas pressure is varied to set the ring radius for pions or kaons or protons at the LD location. The narrow diaphragm mounted in CEDAR-N separates kaons from pions up to 300 GeV/ $c$ , and can tag protons down to 12 GeV/ $c$ .

#### 4.2 Target and target detectors

The target platform is movable and allows easy insertion of a solid target, e.g., a cylindrical lead plate 40 mm in diameter and 1.4 mm thick. We use silicon tracking detectors before and immediately after the targets. These are essential for Primakoff reactions as the angles have to be measured with a precision of order 100  $\mu$ rad. We veto target break-up events via a target recoil detector, and by selecting low- $t$  events in the off-line analysis.

#### 4.3 The $\gamma$ calorimeter ECAL2

The COMPASS  $\gamma$  detector is equipped with 3.8 by 3.8 cm<sup>2</sup> GAMS lead-glass for a total active area of order 2 m diameter. The central area is already completely instrumented with ADC readouts. For the precise monitoring of energy calibration of the photon calorimeters, COMPASS will use LED and laser monitor systems, as described in Ref. [47]. The position resolution in the second  $\gamma$  calorimeter ECAL2 for the photon is 1.0 mm, corresponding to an angular resolution of 30  $\mu$ rad. In the interesting energy range, the energy resolution is 2–3%. The photon acceptance is 98% due to a beam hole of ECAL2, while the reconstruction efficiency is 58%, as a result of pair production within the spectrometer.

As can be seen from Fig. 1, COMPASS requires reconstructed  $\eta$ 's for the hybrid study. The two  $\gamma$ 's from  $\eta$  decay have half-opening angles  $\theta_{\gamma\gamma}^h$  for the symmetric decays of  $\theta_{\gamma\gamma}^h = m/E_\eta$ , where  $m$  is the mass ( $\eta$ ) and  $E_\eta$  is the  $\eta$  energy. (Opening angles are somewhat larger for asymmetric decays.) In order to catch most of the decays, it is necessary to subtend a cone with about double that angle, i.e.,  $\pm 2m/E_\eta$ , neglecting the angular spread of the original  $\eta$ 's around the beam direction. For the ECAL2  $\gamma$  detector, with a circular active area of 2 m in diameter, the acceptance for the  $\pi\eta$  channel at 30 m from the target for  $\eta$ 's above  $E_\eta = 33$  GeV is therefore excellent. At half this energy, however, the acceptance becomes quite poor. The acceptance depends of course on the Hybrid mass, which is taken between 1.4 and 3.0 GeV for the planned COMPASS study. Detailed Monte Carlo studies are needed for different Hybrid decay modes, for a range of assumed masses. For the  $\pi f_1$  channel, for example,  $f_1 \rightarrow \pi\pi\eta$ , the

$\eta$ 's will have low energy, and therefore large  $\gamma$  angles. To maintain good acceptance for low-energy  $\eta$ 's, the ECAL2 diameter should be about 2 m.

The available COMPASS ECAL does not have radiation hardened blocks near the beam hole. If those were available, it would allow increasing the beam intensity by a factor of five, to allow substantially more statistics for the same run time. This would clearly be a cost-effective improvement.

#### 4.4 The magnetic spectrometer and the $t$ -resolution

The  $p_T$  impulses of the COMPASS magnets are 0.3 GeV/ $c$  for SM1 (4 metres from target) and 1.56 GeV/ $c$  for SM2 (16 metres from target). The fields of both magnets are set in the same direction for maximum deflection of the beam. We achieve good momentum resolution for the incident and final-state charged and neutral mesons, and therefore good resolution in  $t$ . The relative momentum resolution for charged  $\pi$ , with all interactions accounted for, is 1% for energies above 35 GeV and up to 2.5% below this mark. The angular resolution in a single coordinate for a charged-pion of momentum  $p$  is 7.9 mrad-GeV/ $p$ . The reconstruction efficiency for pions with energy greater than 2 GeV is 92%.

The angular resolution for a final-state charged meson is controlled by minimizing the multiple scattering in the targets and detectors. With a lead target of 0.8% interaction length (1.6 g/cm<sup>2</sup>, 24% radiation length), multiple Coulomb scattering (MCS) of the beam and outgoing pion in the target gives an rms angular resolution of order 32  $\mu$ rad, small compared to the intrinsic tracking-detector angular resolution. The target contributes to the resolution in the transverse momentum  $p_T$  through MCS. For  $t = p_T^2$ , including all other effects [15, 17], we aim for a  $p_T$  resolution of less than 15 MeV, corresponding to  $\Delta t$  smaller than  $\approx 2.5 \times 10^{-4}$  GeV<sup>2</sup>.

This resolution will provide good separation for contributions from diffractive and meson-exchange processes. Minimum material (radiation and interaction lengths) in COMPASS will also yield a higher acceptance, since the  $\gamma$ 's will not be converted before the ECAL2, and the result is minimum  $e^+e^-$  backgrounds.

#### 4.5 The COMPASS Primakoff trigger

We design [15, 16, 48] the COMPASS Primakoff trigger to enhance the acceptance and statistics. We minimize target break-up events via veto scintillators around the target. The trigger uses the characteristic decay pattern: one or three charged mesons with accompanying  $\gamma$  hits, or three charged mesons and no  $\gamma$  hits. The trigger [15, 16, 48] for the  $\pi\eta$  hybrid decay channel (charged particle multiplicity = 1) is based on a determination of the pion energy loss (via its characteristic angular deflection), correlated with downstream scintillator hodoscopes stations (H1 versus H2) with the aid of a fast matrix chip, as shown in Fig. 2. This trigger is a copy of the currently running muon-beam energy-loss trigger [35]. We will use the Beam Kill detectors BK1/BK2 as veto only during low-intensity tests. These detectors are positioned in the pion-beam trajectory, as shown in Fig. 2, but they cannot handle the full 100 MHz beam rate.

### 5. OBJECTIVES AND EXPECTED SIGNIFICANCE

COMPASS can study pionic hybrid-meson candidates between near 1.4–1.9 GeV, produced by the ultra-peripheral Primakoff reaction. But COMPASS may also be sensitive to pionic and kaonic hybrids for the 1.9–3.0 GeV mass range, if they also couple to the  $\pi\rho$  and  $K\rho$  channels. We can then potentially obtain superior statistics for hybrid states via a production mechanism that is not complicated by hadronic final-state interactions. We can also get important data on the different decay modes in both pionic and kaonic channels.

We make initial rough estimates of the statistics attainable for hybrid production in the COMPASS experiment. Monte Carlo simulations will refine these estimates. We assume a 1.6 mb cross section per Pb nucleus for production of a 1.6 GeV Hybrid meson. We use the radiative width of

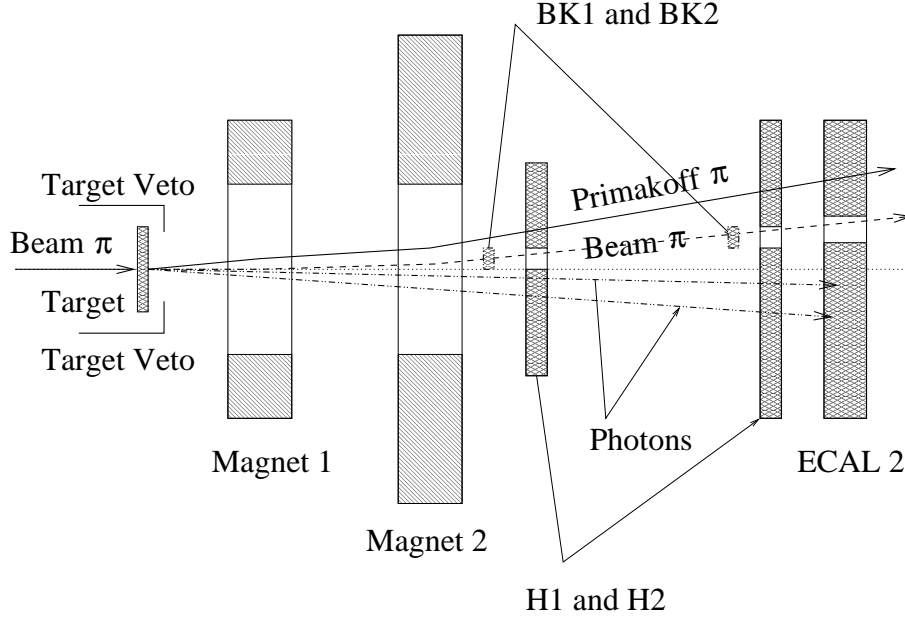


Fig. 2: Detector layout for the COMPASS Primakoff Hybrid trigger,  $\pi^- Z \rightarrow Hybrid \rightarrow \pi^- \eta$ . BK1, BK2: beam killer system; H1, H2: hodoscope system for charged particle detection; ECAL2: second photon calorimeter. For  $\eta$  decay, one observes the two  $\gamma$ 's shown. For polarizability, there is only one  $\gamma$  to detect.

$\Gamma(\pi(1600) \rightarrow \pi\gamma) \approx 1000$  keV, as described above, and also for the 1.9–3.0 GeV mass region. Integrating the Primakoff Hybrid production differential cross section for a 280 GeV pion beam, and using this radiative width, gives 1.6 mb [16, 32, 33].

We consider a beam flux of  $2 \times 10^7$  pions/s, with a spill structure that provides a 5-second beam every 16 seconds. In two months of running at 100% efficiency, we obtain  $3.2 \times 10^{13}$  beam pions. Prior to the data production run, time is also needed to calibrate ECAL2, to make the tracking detectors operational, to bring the DAQ to a stable mode, and for other contingencies. We use a 0.8 % interaction length target, or 1.4 mm lead plate with target density  $N_t = 10^{22}$  cm $^{-2}$ . The Primakoff interaction rate is then  $R = \sigma(Pb) \cdot N_t = 1.6 \times 10^{-5}$ . In a two-month run period, we therefore obtain  $5.1 \times 10^8$  Hybrid events at 100% efficiency. Considering efficiencies for tracking (92%),  $\gamma$  detection (58% for each  $\gamma$ ), accelerator and COMPASS operation (70%), analysis cuts to reduce backgrounds (75%), branching ratio for the  $\eta \rightarrow 2\gamma$  and  $\eta \rightarrow \pi^+\pi^-\pi^0$  decay modes ( $\approx 62\%$ ), trigger efficiency ( $\approx 60\%$ ), geometrical acceptances ( $\approx 90\%$ ),  $\pi^0$  and  $\eta$  reconstruction from two  $\gamma$  hits ( $\approx 45\%$ ), and event reconstruction efficiencies ( $\approx 60\%$ ), we estimate a global efficiency of  $\epsilon(\text{total}) = 1.5\%$ . We will assume here the same average detection efficiency for all Hybrid decay modes, via  $\rho\pi, \eta\pi, \eta'\pi, \pi b_1, \pi f_1$ . Therefore, we can expect to observe a total of  $7.7 \times 10^6$  Hybrid decays in all decay channels for the 1.6 GeV Hybrid. For example, following theory and VES branching ratios, we expect for the 1.6 GeV state, most data in the  $\pi f_1, \pi\rho, \pi\eta'$ , and  $b_1\pi$  channels.

For 2, 2.5, 3.0 GeV mass Hybrids, assuming that they have the same radiative width, the number of useful events decreases by factors of 6, 25, and 100, respectively. But even in these cases, assuming again a global 1.5% efficiency, that would represent a very interesting potential of samples of  $13 \times 10^5$ ,  $3.1 \times 10^5$ , and  $0.77 \times 10^5$  Hybrid meson detected events, with masses 2.0, 2.5, and 3.0 GeV, respectively.

Taking into account the very high beam intensity, fast data acquisition, high acceptance and good resolution of the COMPASS set-up, one can expect from COMPASS the highest statistics and a ‘systematics-free’ data sample that includes many tests to control possible uncertainties. Comparison between COMPASS and past and new experiments [6, 8], with complementary methodologies, should



allow fast progress on understanding Hybrid meson structure, their production and decay characteristics, and on establishing systematic uncertainties.

### Acknowledgements

This work was supported in part by the Israel Science Foundation funded by the Israel Academy of Sciences and Humanities. Thanks are due to T. Ferbel, V. Dorofeev, and S. Paul for a critical reading of this manuscript. Thanks are due also to R. Bertini, F. Bradamante, A. Bravar, D. Casey, S. U. Chung, M. Colantoni, N. d'Hose, S. Donskov, W. Dunnweber, M. Faessler, M. Finger, L. Frankfurt, S. Godfrey, H. Hahn, D. von Harrach, T. Hasegawa, Y. Khokhlov, K. Königsmann, R. Kuhn, F. Kunne, L. Landsberg, J. Lichtenstadt, A. Magnon, G. Mallot, V. Molchanov, J. Nassalski, A. Olchevski, E. Piasetzky, J. Pochodzalla, S. Prakhov, A. Sandacz, L. Schmitt, C. Schwarz, H. W. Siebert, V. Sougoniaev, T. Walcher, and M. Zielinski for valuable discussions. Thanks are due to the Johannes Gutenberg University (Mainz, Germany) for hospitality during the writing of this report, during a sabbatical leave from Tel Aviv University, as a visiting Mercator Professor.

### References

- [1] N. Isgur and A. Dzierba, CERN Courier **40** (2000) 23;  
<http://www.cerncourier.com/main/article/40/7/16>.
- [2] A. Dzierba *et al.*, Amer. Sci. **88** (2000) 406;  
<http://www.americanscientist.org/articles/00articles/dzierba.html>;  
QCD Confinement and the Hall D Project at Jefferson Lab, hep-ex/0106010.
- [3] S. Godfrey and J. Napolitano, Rev. Mod. Phys. **71** (1999) 1411; hep-ph/0211464, these proceedings.
- [4] S. U. Chung, Nucl. Phys. B **86** (2000) 341.
- [5] W. Dünnweber, these proceedings.
- [6] U. Wiedner, Exotic Meson Prospects via a New Facility for  $p\bar{p}$  reactions,  
[www.gsi.de/GSI-Future/program.html](http://www.gsi.de/GSI-Future/program.html), Darmstadt, Germany, Oct. 2000, Light-Quark Spectroscopy with Anti-Proton Proton Annihilation, Workshop on Low-Energy Pbar Storage Ring (Pbar2000), Aug. 2000, Chicago, Illinois, <http://www.iit.edu/bcps/hep/pbar2000.html>.
- [7] A. Dzierba *et al.*, The Hall D project Design Report, Searching for QCD Exotics with a Beam of Photons, Nov. 2000; <http://dustbunny.physics.indiana.edu/HallD/>.
- [8] S. U. Chung, Exotic Meson Prospects via FNAL CDF/D0 and BNL RICH double-Pomeron production, private communication.
- [9] A. Abele *et al.*, Phys. Lett. B **423** (1998) 175.
- [10] D. R. Thompson *et al.*, Phys. Rev. Lett. **79** (1997) 1630; G. S. Adams *et al.*, Phys. Rev. Lett. **81** (1998) 5760; S. U. Chung *et al.*, Phys. Rev. D **65** (2002) 072001.
- [11] V. Dorofeev (VES Collaboration), hep-ex/9905002, hep-ex/0110075; I Kachaev, hep-ex/0111067; A. Zaitsev, Nucl. Phys. A **675** (2000) 155c.
- [12] S. Donskov, these proceedings.
- [13] V. Dorofeev, these proceedings.

- [14] CERN Proposal COMPASS, <http://wwwcompass.cern.ch/>, CERN/SPSLC 96-14, SPSC/P297; CERN/SPSLC 96-30, SPSC/P297, Addendum 1; <http://www-nuclear.tau.ac.il/~murraym/primaphysreps.html>
- [15] M. A. Moinester, V. Steiner and S. Prakhov, Hadron-Photon Interactions in COMPASS, hep-ph/9910039.
- [16] M. A. Moinester and S. U. Chung, Hybrid Meson Structure at COMPASS, hep-ex/0003008.
- [17] M. A. Moinester, Pion Polarizabilities and Hybrid Meson Structure at COMPASS, hep-ex/0012063.
- [18] S. U. Chung, E. Klempt and J. Koerner, hep-ph/0211100.
- [19] A. Donnachie and P. R. Page, Phys. Rev. D **58** (1998) 114012.
- [20] S. Bass, hep-ph/0210018.
- [21] T. Barnes, Photoproduction of Hybrid Mesons, nucl-th/9907020; Hadron 2001 Conference Summary, hep-ph/0202157.
- [22] N. Isgur, Phys. Rev. D **60** (1999) 114016.
- [23] F. Close and P. Page, Nucl. Phys. B **443** (1995) 233.
- [24] N. Isgur, Spectroscopy - An Introduction and Overview, JLAB-THY-99-03-A, Feb 1999, in Proceedings of the 8th International Conference on the Structure of Baryons (Baryons 98), Bonn, Germany, Sept. 1998, Eds. D. W. Menze, B. Metsch, World Scientific, 1999.
- [25] K. Peters, Meson Spectroscopy and Exotic Quantum Numbers, in Proceedings of the 8th International Conference on the Structure of Baryons (Baryons 98), Bonn, Germany, Sept. 1998, Eds. D. W. Menze, B. Metsch, World Scientific, 1999; Physics of Exotic and Non-Exotic Mesons at HESR, Workshop on Gross Properties of Nuclei and Nuclear Excitations, Hirschegg, Austria, Jan 2001, <http://theory.gsi.de/hirschegg/>.
- [26] D. Alde *et al.*, Proc. of HADRON-97, BNL, August 1997.
- [27] Yu.D. Prokoshkin and S.A. Sadovsky, Phys. At. Nucl. **58** (1995) 606.
- [28] G. M. Beliadze *et al.*, Phys. Lett. B **313** (1993) 276–282; A.Zaitsev, Proc. of HADRON-97, BNL, August 1997.
- [29] D. Alde *et al.*, Phys. Lett. B **205** (1988) 397; Phys. Atom. Nucl. **62** (1999) 1993.
- [30] H. Aoyagi *et al.*, Phys. Lett. B **314** (1993) 246.
- [31] T. Jensen *et al.*, Phys. Rev. **27D** (1983) 26.
- [32] M. Zielinski *et al.*, Z. Phys. C **31** (1986) 545; Z. Phys. C **34** (1987) 255; M. Zielinski (in BNL 88, Glueballs, Hybrids, and Exotic Hadrons); M. Zielinski, Acta Phys. Polon. B **18** (1987) 455.
- [33] T. Ferbel *et al.*, Proceedings of the XVIth Rencontre de Moriond on New Flavors and Hadron Spectroscopy, Les Arcs, Savoie, 1981, p. 373; Acta Phys. Polon. B **12** (1981) 1129.
- [34] V. Molchonov *et al.* (SELEX Collaboration), Phys. Lett. **B521** (2001) 171.
- [35] CERN Workshop on Future Physics at COMPASS, Sept. 2002, Proceedings and Transparencies, <http://compass-cw2002.web.cern.ch/compass-cw2002/programme.htm>.

- [36] M. Zielinski *et al.*, *Z. Phys. C, Particles and Fields* **16** (1983) 197.
- [37] G. T. Condo *et al.*, *Phys. Rev.* **43D** (1991) 2787.
- [38] S. U. Chung, Future Prospects for Exotic Mesons, Workshop on Gross Properties of Nuclei and Nuclear Excitations, Hirschegg, Austria, Jan 2001, <http://theory.gsi.de/hirschegg/>.
- [39] J. Huston *et al.*, *Phys. Rev.* **33** (1986) 3199.
- [40] L. Capraro *et al.*, *Nucl. Phys. B* **288** (1987) 659.
- [41] M. Zielinski *et al.*, *Phys. Rev. Lett.* **52** (1984) 1195.
- [42] S. Cihangir *et al.*, *Phys. Lett.* **117B** (1982) 119; *ibid.*, p.123; *Phys. Rev. Lett.* **51** (1983) 1.
- [43] D. Berg *et al.*, *Phys. Lett. B* **98** (1981) 119.
- [44] C. Chandlee *et al.*, *Phys. Rev. Lett.* **51** (1983) 168.
- [45] H. W. Atherton *et al.*, Precise Measurements of Particle Production by 400 GeV/c Protons on Beryllium Targets, report CERN 80-07, 1980.
- [46] M. Benot *et al.*, *Nucl. Instr. Meth.* **105** (1972) 431; C. Bovet, S. Milner and A. Placci, CERN/Lab. II/EA/74-4, (Rev. Aug 1975), The CEDAR Project; Cerenkov Differential counters with Achromatic Ring focus; C. Bovet *et al.*, CERN-SPS/EBP/77-19, The CEDAR Project, *IEEE Trans. Nucl. Sci.* **25** (1978) 572; C. Bovet *et al.*, CERN report CERN 82-13, The CEDAR counters for particle identification in the SPS secondary beams: a description and operation manual.
- [47] M. Moinester, [http://www-nuclear.tau.ac.il/~murraym/COMPASS/laser\\_monitor\\_techrep.html](http://www-nuclear.tau.ac.il/~murraym/COMPASS/laser_monitor_techrep.html).
- [48] M. A. Moinester and V. Steiner, Pion and Kaon Polarizabilities and Radiative Transitions, Proc. 'Chiral Dynamics Workshop' U. Mainz, Sept. 1997, hep-ex/9801008.